Fractional-Bits per Symbol Using Non-Powers-of-2-Point Constellations

Benjamin J. Wedemire
ben.wedemire@ieee.org
University of New Brunswick
Fredericton, New Brunswick, Canada

Brent R. Petersen
University of New Brunswick
Fredericton, New Brunswick, Canada

ABSTRACT

Radios operating in a slowly fading channel require adaptive communication links that adjust to channel conditions that are not always ideal. Matching a communication link's bit rate to the channel conditions is critical to maximize throughput. A fractional-bits per symbol communication systems is discussed as a possible method to better adapt to channel conditions. Sequences of constellations containing non-powers-of-2-points are used to facilitate the fractional-bits per symbol system and create multi-symbol waveforms. Equations governing sequences are described. Mapping schemes are explored as a method of mapping waveforms to binary strings. The relationship between sequence properties, length, number of points, and waveform utilization efficiency, are shown to affect the bit error rate.

CCS CONCEPTS

• **Hardware** → *Wireless devices*; **Digital signal processing**; • **Networks** → **Link-layer protocols**.

KEYWORDS

Communications, Adaptive Modulation, Adaptive Coded Modulation, Fractional-Bits, N-Point Constellations, Satellites, LEO, CubeSat

ACM Reference Format:
Benjamin J. Wedemire and Brent R. Petersen. 2021. Fractional-Bits per Symbol Using Non-Powers-of-2-Point Constellations. In *ICTRS 2021, Tenth International Conference on Telecommunications and Remote Sensing, November 15–16, 2021, Sofia, Bulgaria.* ACM, New York, NY, USA, 5 pages. https://doi.org/10.1145/3495535.3495540

1 INTRODUCTION

When designing radio links for use on a satellite, designers generally use the worst-case link scenario in link budget calculations to ensure that the link operates under all conditions at a specified rate. For satellite links that do not experience significant fading this is acceptable, however for satellites that do experience fading this results in inefficient communication links. Fading can be caused by changing distance between the transmitter and receiver, rain, scintillation, multipath, humidity, temperature variations, increased noise from nearby transmitters, or other natural or man-made phenomena [11].

In the case of satellites in a low-earth orbit (LEO), a major fading event occurs during every pass over a ground station (GS). The fading event occurs because the orbital period of the satellite is not the same as the Earth's rotational period which results in a dramatic change in distance between the satellite and the GS. With LEO satellites becoming more common, determining how radios onboard these satellites overcome fading while maintaining efficient radio links is a major design decision [7, 9, 13].

For the CubeSat VIOLET, a satellite in the nanosatellite (1-10 kg) category built by CubeSat New Brunswick (CNB), the range between the spacecraft and the GS will be approximately 400 km to 2400 km. VIOLET is an energy, power, and computational resource constrained satellite and requires a low-power and computationally inexpensive communication system that radiates into the S band. An additional challenge for VIOLET's communication system is the amount of data that the two science missions on-board VIOLET generate to be downloaded each day. The first mission, GNSS Receiver for Ionospheric and Position Studies (GRIPS), will use a Global Navigation Satellite System (GNSS) receiver to record raw multi-constellation, multi-frequency GNSS observations. The second mission, Spectral Airglow Structure Imager (SASI), will take images of the airglow produced within the ionosphere from the photon emission of atomic oxygen at 630 nm. Together, these missions produce approximately 500 MB of data per day.

One method of overcoming the fading effects is to apply an error correcting code that has the ability to adjust the amount of error correcting information in the transmission [10]. An example of this is a system using punctured codes to adapt the coding rate to the channel conditions [12]. This approach is powerful at combating fading at the expense of more computation resources than uncoded communication systems. A different approach changes the selected constellation based on current channel conditions [4]. An example system using a phase-shift keying (PSK) modulation scheme might select between binary PSK (BPSK), quadrature PSK (QPSK), and 8-PSK. This system can also adapts to channel fading but it is not always possible to select a constellation that best matches the channel conditions. Still, other systems combine these two techniques [1, 2].

To improve the ability to match the bit-rate to the channel conditions with a computationally inexpensive and low-power system, this paper introduces a communication system that uses constellations that contain a number of points that are non-powers-of-two. This creates fractional-bits per symbol. Previously, a description of constellations containing non-powers-of-two numbers of points has been presented but no implementation method has been provided [8]. To achieve fractional-bits per symbol, sequences are introduces which are used to facilitate a whole number of bits to be transmitted per sequence period. Additionally, adaptive coding and modulation (ACM) [3, 5, 6] could be used to switch between sequences and mapping schemes using channel state information

Accepted Manuscript
ICTRS 2021, November 15–16, 2021, Sofia, Bulgaria
2021. ACM ISBN 978-1-4503-9018-7/21/11…$15.00
https://doi.org/10.1145/3495535.3495540

(CSI). This allows for the bit rate to be adjusted as the channel conditions change. The use of sequences could allow for a better match between the channel conditions and the bit rate which, in future communication systems, could better utilize the radio spectrum resource. The organization of this paper is as follows: section 2 introduces sequences and the implications of using them; section 3 examines bit-to-waveform mapping; section 4 introduces the simulation that was developed to characterize the performance of the fractional-bit rate systems and the simulation results; finally, in section 5, conclusions are drawn from the results and future work is presented.

2 SEQUENCES

Sequences are the basis for this fractional bit-rate system; they define a whole number of symbols which are grouped together where each element in the sequence represents the number of constellation points that are available to be selected from during each symbol period. The mathematical representation of a sequence is described as:

$$S = [s_1, s_2, \dots, s_N], \tag{1}$$

where S is the sequence in use and the elements describe the number of constellation points that are available during each symbol period of S. N defines the length or number of symbols contained in one sequence. Sequences do not require a specific modulation scheme to be used during transmission but the authors propose four basic rules for using sequences. Rule one, sequences are sequential, each position is in the sequence selected in the order they appear in the sequence. Second, sequences repeat, once the end of the sequence is reached the sequence restarts by re-selecting the constellation at the first position. Third, sequences can require switching between constellations from one symbol period to the next. Fourth, it is proposed to define the bit rate of the selected sequence not by how many bits are transmitted per symbol but by how many are transmitted per waveform, where a waveform is described as the unique pattern created by selecting a symbol at each symbol period determined by the sequence. To determine the number of bits per waveform, the number of unique waveforms needs to be determined,

$$W_{[s_1,s_2,\dots,s_N]} = \prod_{n=1}^{N} s_n. \tag{2}$$

$W_{[s_1,s_2,\dots,s_N]}$ describes the number of unique waveforms contained in the set $W_{A[s_1,s_2,\dots,s_N]}$, where $W_{A[s_1,s_2,\dots,s_N]}$ is generated by expanding sequence S and is of size $W_{[s_1,s_2,\dots,s_N]}$ by N. $W_{Ai[s_1,s_2,\dots,s_N]}$ is one unique waveform located at row i of $W_{A[s_1,s_2,\dots,s_N]}$ and contains the symbols $(i,1),(i,2),\dots(i,N)$. The maximum number of bits contained in a unique waveform is then given by:

$$b_{[s_1,s_2,\dots,s_N]} = \left\lfloor \log_2(W_{[s_1,s_2,\dots,s_N]}) \right\rfloor, \tag{3}$$

where $b_{[s_1,s_2,\dots,s_N]}$ is the whole number of bits that can be transmitted with a waveform generated from S. By flooring $W_{[s_1,s_2,\dots,s_N]}$ this implies that there may be more than a power of two unique waveforms. This is true and means that some waveforms will not be mapped. The number of waveforms that will be mapped is given by:

$$W'_{[s_1,s_2,\dots,s_N]} = 2^{b_{[s_1,s_2,\dots,s_N]}}. \tag{4}$$

$W'_{[s_1,s_2,\dots,s_N]}$ is used to describe length of the subset of waveforms that will be selected from $W_{A[s_1,s_2,\dots,s_N]}$ by a mapping process. Additionally, $W''_{[s_1,s_2,\dots,s_N]}$ is used to describe the number of waveforms that will not be selected in the mapping process and is defined by:

$$W''_{[s_1,s_2,\dots,s_N]} = W_{[s_1,s_2,\dots,s_N]} - W'_{[s_1,s_2,\dots,s_N]}. \tag{5}$$

The waveform utilization efficiency of a sequence, $\eta_{[s_1,s_2,\dots,s_N]}$, describes what percentage of the total number of possible waveforms is used. It is defined as:

$$\eta_{[s_1,s_2,\dots,s_N]} = \frac{W'_{[s_1,s_2,\dots,s_N]}}{W_{[s_1,s_2,\dots,s_N]}} 100\%. \tag{6}$$

3 MAPPING

Waveform mapping is an important consideration with this fractional-bit rate system because, generally, $W_{[s_1,s_2,\dots,s_N]}$ is not equal to $W'_{[s_1,s_2,\dots,s_N]}$. This results in selecting $W'_{[s_1,s_2,\dots,s_N]}$ waveforms out of the total set of waveforms, $W_{A[s_1,s_2,\dots,s_N]}$. The mapped subset of waveforms through a mapping process is $W_{M[s_1,s_2,\dots,s_N]}$ and the unmapped subset of waveforms is $W_{U[s_1,s_2,\dots,s_N]}$. Generally, $W_{M[s_1,s_2,\dots,s_N]}$ are the indices 1 to $W'_{[s_1,s_2,\dots,s_N]}$ of $W_{A[s_1,s_2,\dots,s_N]}$ and $W_{U[s_1,s_2,\dots,s_N]}$ are indices $W'_{[s_1,s_2,\dots,s_N]} + 1$ to $W_{[s_1,s_2,\dots,s_N]}$ of $W_{A[s_1,s_2,\dots,s_N]}$.

Two mapping schemes are proposed with each scheme being of varying complexity and optimization. The two mapping schemes are linear and random mapping. It is noted that these mapping schemes are by-no-means the only mapping schemes. Other schemes are possible and some may be capable of better performance with relatively low computational complexity. The result of the mapping process is two lookup tables (LUT). One LUT is called the TX LUT, located at the transmitter, and the other is called the RX LUT, located at the receiver. The TX LUT is used to convert binary strings into the waveforms used for transmissions and is of size 1 by $W_{[s_1,s_2,\dots,s_N]}$. The RX LUT is used to demap the received waveforms back to binary strings once received and is of size $b_{[s_1,s_2,\dots,s_N]} + 1$ by $W_{[s_1,s_2,\dots,s_N]}$ matrix. After the RX LUT generation is complete, the RX LUT is truncated to a $b_{[s_1,s_2,\dots,s_N]}$ by $W_{[s_1,s_2,\dots,s_N]}$. The advantage of this method is that the mapping process is performed before the system is used and therefore the task of generating the LUTs is not performed by the communication system. The communication system only needs to use the LUT during operation. Examples of these LUTs are provided by Table 1 and Table 2 using decimals to represent binary strings.

Table 1: Example of a TX LUT

TX LUT for Sequence [3 4]						
Index	1	2	3	4	5	6
$W_{A[3,4]}$	W_{A1}	W_{A2}	W_{A3}	W_{A4}	W_{A5}	W_{A6}
Index	7	8	9	10	11	12
$W_{A[3,4]}$	W_{A7}	W_{A8}	W_{A9}	W_{A10}	W_{A11}	W_{A12}

3.1 Linear

A linear mapping scheme is the simplest mapping scheme. It requires little computational complexity and therefore a simplified

Table 2: Example of a RX LUT

RX LUT for Sequence [3 4]						
Index	W_{A1}	W_{A2}	W_{A3}	W_{A4}	W_{A5}	W_{A6}
Data	D_1	D_2	D_3	D_4	D_5	D_6
Index	W_{A7}	W_{A8}	W_{A9}	W_{A10}	$W_{A11}1$	W_{A12}
Data	D_7	D_8	D_9	D_{10}	D_{11}	D_{12}

LUT generation. To perform linear mapping, the TX LUT and RX LUT can be generated in parallel and both are length $W_{[s_1,s_2,\ldots,s_N]}$. For generation of the TX LUT, indices of the TX LUT are the decimal representation, plus one, of the binary data to be sent and the numbers stored at each index is the waveform used to represent that binary string. To perform linear mapping of the TX LUT, the first index is mapped to the first waveform, $W_{A1[s_1,s_2,\ldots,s_N]}$, in the set of $W_{A[s_1,s_2,\ldots,s_N]}$, the second index is mapped to the second waveform, $W_{A2[s_1,s_2,\ldots,s_N]}$, and so on until index $W_{[s_1,s_2,\ldots,s_N]}$ is mapped to the waveform at position $W_{[s_1,s_2,\ldots,s_N]}$. The process is repeated for the RX LUT but the indices the RX LUT represents the received waveform and values contained in the RX LUT are the binary values of the data that was transmitted. To perform linear mapping of the RX LUT, the first index is mapped to the binary string D_1, the second index is mapped to D_2, and so on until index $W_{[s_1,s_2,\ldots,s_N]}$ is mapped to the binary string D_W. The valid subset, $W_{M[s_1,s_2,\ldots,s_N]}$, occurs in the range of indices 1 to $W'_{[s_1,s_2,\ldots,s_N]}$ and invalid subset $W_{U[s_1,s_2,\ldots,s_N]}$ occurs in the range of indices $W'_{[s_1,s_2,\ldots,s_N]}+1$ to $W_{[s_1,s_2,\ldots,s_N]}$ of $W_{A[s_1,s_2,\ldots,s_N]}$. A disadvantage of this mapping scheme is that constellation points at certain positions of the sequence may not have an equal probability compared to other constellation points. An example of this is with the sequence [3 3 3]. Waveform $W_{A1[3,3,3]}$ or [0 0 0] will be mapped to index 1, waveform [0 0 1] will be mapped to index 2, waveform [0 0 2] will be mapped to index 3, waveform [0 1 0] will be mapped to index 4 and so on till waveform [2 2 2] is mapped to index 27. The last valid waveform is located at index $W'_{[3,3,3]}$ of $W_{[3,3,3]}$ and is waveform [1 2 0]. It results in s_1 of only using symbols 0 and 1 during operation. As a result, symbols at position s_1 do not have the equal probabilities. Symbols may still appear as symbol 2 at the receiver but only when errors occur. A problem arises when a waveform is received from the subset of $W_{U[s_1,s_2,\ldots,s_N]}$. When this occurs, an incorrect bit string will be received and bit errors result.

3.2 Random

Similar to linear mapping, random mapping requires little computation complexity, however it overcomes the problem of equal probability of constellation points at all sequence positions. To perform random mapping, either the TX LUT is generated then converted to the RX LUT or vice versa. To perform random mapping by first generating the TX LUT, the mapping process assigns the values of 1 to $W_{[s_1,s_2,\ldots,s_N]}$ randomly to indices in the TX LUT. In an example where $S = [3, 3, 3]$, index 1 of the TX LUT might be mapped to waveform [1 0 2], index 2 might be mapped to waveform [0 2 1], index 3 might be mapped to [0 1 1], and so on. The TX LUT then contains valid waveforms within indices 1 to $W'_{[s_1,s_2,\ldots,s_N]}$ and non-valid waveforms within indices $W'_{[s_1,s_2,\ldots,s_N]}+1$ to $W_{[s_1,s_2,\ldots,s_N]}$.

To generate the RX LUT from the TX LUT, a search is performed on the values in the TX LUT to find which waveform is mapped to each binary value. The binary vales are copied back to the RX LUT. This mapping process generally, overcomes issues with linear mapping and non-equal probability symbols. A problem arises when a waveform is received from the subset of $W_{U[s_1,s_2,\ldots,s_N]}$. When this occurs, an incorrect bit string will be received and bit errors result.

4 SIMULATION

A Monte-Carlo simulation has been created in MATLAB® to determine the bit error rate (BER) of the fractional-bit rate system using various sequences. Simulations were run to determine the effects of changing the number of points at a given position in the sequence, sequence length, and waveform utilization efficiency. Additionally, the performance of this fractional-bit rate system was compared to traditional, non-fractional-bit rate communication systems. For each simulation, a minimum of 1000 bit errors were counted. The non-fractional and fractional communication system simulations use the phase-shift keying modulation scheme. The non-fractional system uses BPSK, QPSK, and 8-PSK constellations. The fractional system uses a PSK constellation containing two through eight points. These constellations contain all points on a unit circle with radius one. The angle between the positive real-axis and the point is defined using this equation:

$$\angle C_p = \frac{p\,360^\circ}{P}, \tag{7}$$

where C_p is the constellation point in question, p is the index of the point counted from a counter-clockwise angle between the positive real axis, and P is the total number of points within the constellation. Finally, to calculate the signal-to-noise ratio (SNR), the number of bits per symbol must be calculated. For a non-fractional-bit rate system, the number of bits per symbol is given by:

$$B = \log_2(P), \tag{8}$$

where B is the number of bits per symbol and P is the number of points in the constellation. For a fractional-bit rate system, two definitions of how much information is transmitted in one waveform period could be used. The first method gives the actual number of bits per symbol given by:

$$B = \frac{b_{[s_1,s_2,\ldots,s_N]}}{N}. \tag{9}$$

The second method gives the theoretical number of bits per symbol given by:

$$B = \frac{\log_2(W_{[s_1,s_2,\ldots,s_N]})}{N}. \tag{10}$$

In Komo et. al, method two is used for this calculation, however in this paper, method one is used.

4.1 Mappings

Figure 1 shows the simulations results of comparing the linear and random mapping schemes. Both mapping scheme performed similarly, however the randomly mapped is better at creating equal probabilities for all symbols. As a result, the remainder of the simulations were run utilizing the random mapping scheme.

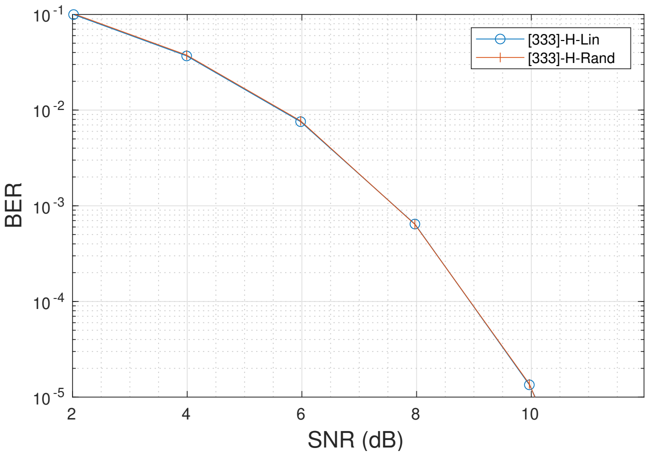

Figure 1: Mapping Scheme Comparison

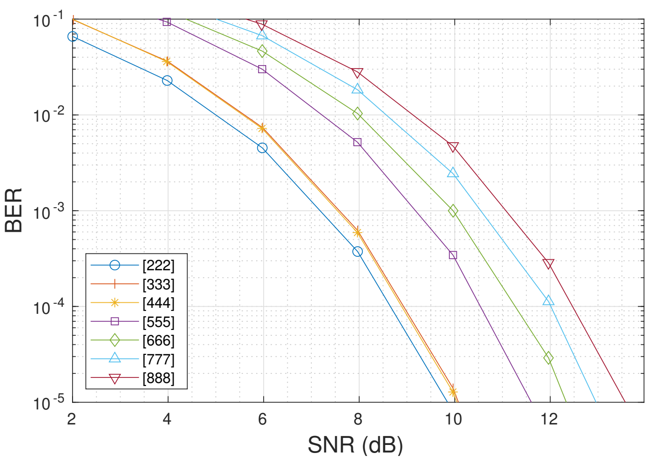

Figure 2: Number of Constellation Points Comparison

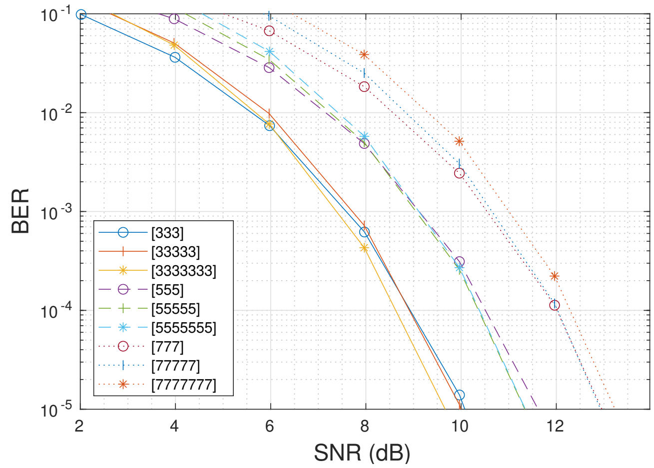

Figure 3: Sequence Length Comparison

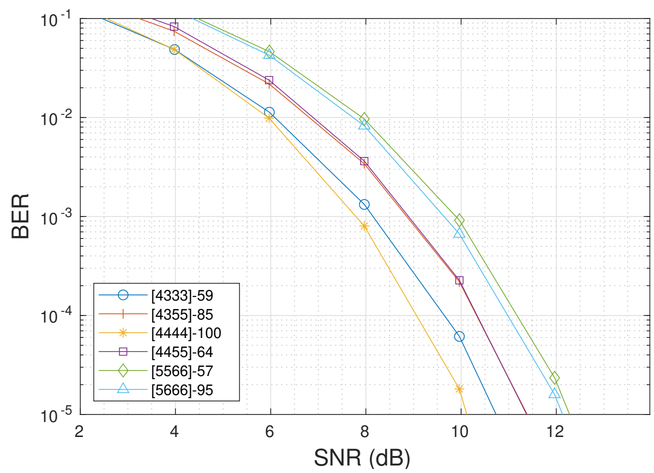

Figure 4: Sequence Efficiency Comparison

4.2 Number of Points

Figure 2 displays the simulation results of comparing length 3 sequences with varying numbers of points within their constellations. The results of the BER versus SNR curves show the expected result that as the number of points in the constellation increases so do the SNR requirements for each new sequence.

4.3 Sequence Length

Figure 3 displays the simulation results of comparing the BER curves found by changing the sequence length of three base sequences, [3 3 3], [5 5 5], and [7 7 7] from length 3, to length 5, and to length 7. The plots show that at low BERs, longer length sequences perform worse then their shorter counterparts. As the SNR improves, longer sequence began to lose bit errors faster than the shorter length sequences.

4.4 Sequence Efficiency

Figure 4 shows the simulation results of six sequences and the effect that the waveform utilization efficiency has on a sequences performance. Waveform utilization efficiencies are presented in the legend of the figure.

4.5 Fractional Versus Non-fractional Communication System

Figure 5 shows the simulation results of comparing a traditional communication system. The fractional-bit rate system uses sequences of varying number of points within their constellations, but all sequences are of length 2. These results show that between communication systems using QPSK and 8-PSK, the sequences [5 5] and [6 6] are viable. However, the sequence [5 5] transmits a number of bits per waveform period of $b_{[5,5]} = 4$ which has the same number of bits as two QPSK symbols. This means that QPSK performs better then the [5 5] sequence and leaves the [6 6] sequence as a viable choice.

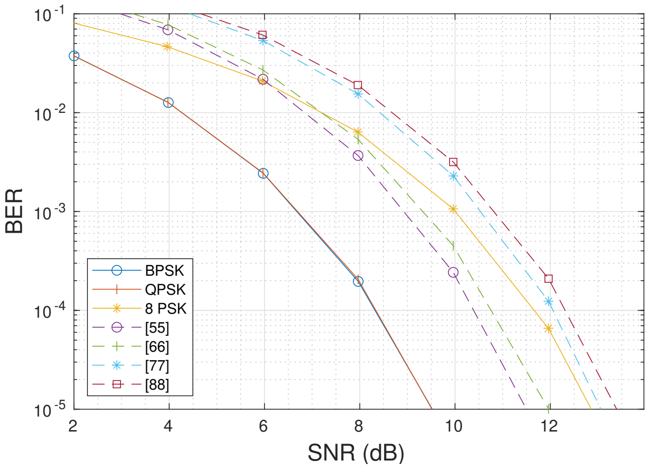

Figure 5: Fractional versus Non-fractional Communication System Comparison

4.6 Throughput

VIOLET is expected to be in communication range of the GS for approximately 30 minutes per day. To compare the throughput of non-fractional and fractional systems, three systems have been calculated in an orbit similar to VIOLET's. The first is a non-fractional static (NS) communication system that uses QPSK. The second is a non-fractional adaptive system (NA), that can pick either QPSK, or 8-PSK depending on the CSI. The third system is a fractional adaptive system (FA) that can pick between QPSK, the sequence [6 6], or 8-PSK depending on the CSI. The assumptions made for this calculation are: an average pass over a GS in Fredericton using the International Space Station's orbit, a symbol rate of 1 Msymbol per second, a maximum BER of 10^{-4}, no other fading sources exist, CSI is perfect and delay-free, the communication system transmits continuously, and the time to change modulation schemes is small and therefore is not noticeable. Table 3 shows the results of comparing three communications systems. The best performing system is the fractional-bit rate system but only by a small margin compared to the non-fractional-bit rate adaptive system.

Table 3: Throughput of Various Communication Systems

System	bits per symbol	NS (s)	NS (Mb)	NA (s)	NA (Mb)	FA (s)	FA (Mb)
QPSK	2	323	646	152	304	109	218
$S = [6\ 6]$	2.5	-	-	-	-	43	108
8-PSK	3	-	-	171	513	171	513
Total	-	323	646	323	817	323	839

5 CONCLUSION

In this paper, a fractional-bit per symbol communication system was introduced. It uses sequences and a mapping scheme to map binary strings to waveforms rather than mapping binary strings to individual symbols as is done in traditional, non-fractional-bit rate communication systems. Two mapping schemes, linear and random were introduced and their characteristics were discussed. A simulation was constructed which allowed for the performance of some sequences available in the fractional-bit per symbol system to be explored. These results were used to determine the effect that certain properties, sequence length, number of points, and the waveform utilization efficiency, have on candidate sequences. The fractional-bit per symbol communication system was also compared against a traditional communication system.

In the future, more mapping schemes should be explored that exploit the set of available waveforms to a greater extent, different decision techniques should be examined, and a physical system should be developed to corroborate the results presented here.

ACKNOWLEDGMENTS

To CubeSat NB, for constant support. To the Canadian Space Agency (CSA), for envisioning the Canadian CubeSat Project (CCP) and funding this research. To the New Brunswick Innovation Foundation (NBIF), for funding this research.

REFERENCES

[1] ETSI. 2014. EN 302 307-1: Digital Video Broadcasting (DVB); Second generation framing structure, channel coding and modulation systems for Broadcasting, Interactive Services, News Gathering and other broadband satellite applications; Part 1: DVB-S2.
[2] ETSI. 2021. EN 302 307-2: Digital Video Broadcasting (DVB); Second generation framing structure, channel coding and modulation systems for Broadcasting, Interactive Services, News Gathering and other broadband satellite applications; Part 2: DVB-S2 Extensions (DVB-S2X).
[3] D.L. Goeckel. 1999. Adaptive coding for time-varying channels using outdated fading estimates. *IEEE Transactions on Communications* 47, 6 (June 1999), 844–855. https://doi.org/10.1109/26.771341
[4] A. Goldsmith. 1999. Adaptive modulation and coding for fading channels. In *Proceedings of the 1999 IEEE Information Theory and Communications Workshop (Cat. No. 99EX253)*. Kruger National Park, South Africa, 24–26. https://doi.org/10.1109/ITCOM.1999.781396
[5] J. Hayes. 1968. Adaptive Feedback Communications. *IEEE Transactions on Communication Technology* 16, 1 (Feb. 1968), 29–34. https://doi.org/10.1109/TCOM.1968.1089811
[6] R. He, D. Yang, H. Wang, and J. Kuang. 2019. Adaptive hierarchical coding and modulation scheme over satellite channels. *IET Communications* 13, 17 (2019), 2834–2839. https://doi.org/10.1049/iet-com.2018.5144
[7] Mehdi Hosseini, Mohammad Hakkak, and Pejman Rezaei. 2010. Adaptive bit rate scheme for a LEO satellite link. In *2010 18th Iranian Conference on Electrical Engineering*. Isfahan, Iran, 200–203. https://doi.org/10.1109/IRANIANCEE.2010.5507519 ISSN: 2164-7054.
[8] J.J. Komo and W.J. Reid. 1991. Evaluation of three- and five-phase PSK. In *IEEE Proceedings of the SOUTHEASTCON '91*. Williamsburg, VA, United States of America, 1030–1033 vol.2. https://doi.org/10.1109/SECON.1991.147918
[9] C.H. Lee. 1995. Variable data rate modem for low Earth orbiting satellite (LEOS) communication. In *Proceedings of MILCOM '95*, Vol. 3. San Diego, CA, United States of America, 1234–1238 vol.3. https://doi.org/10.1109/MILCOM.1995.483692
[10] S. Lin and D.J. Costello. 2004. *Error Control Coding: Fundamentals and Applications* (2nd ed.). Prentice-Hall, Englewood Cliffs, NJ, United States of America.
[11] John G. Proakis and Masoud. Salehi. 2008. *Digital communications* (5th ed.). McGraw-Hill, Boston, MA, United States of America.
[12] P. Robertson and T. Worz. 1998. Bandwidth-efficient turbo trellis-coded modulation using punctured component codes. *IEEE Journal on Selected Areas in Communications* 16, 2 (Feb. 1998), 206–218. https://doi.org/10.1109/49.661109
[13] Nikolaos Toptsidis, Pantelis-Daniel Arapoglou, and Massimo Bertinelli. 2012. Link adaptation for Ka band low Earth orbit Earth Observation systems: A realistic performance assessment. *International Journal of Satellite Communications and Networking* 30, 3 (2012), 131–146. https://doi.org/10.1002/sat.1002